

University of Alabama in Huntsville

**LOUIS**

---

Honors Capstone Projects and Theses

Honors College

---

4-28-2024

## Mining Optical Narrow-Band Imaging Data to Study AGN Feedback and Galaxy Evolution

Dakota Michael Davis

*University of Alabama in Huntsville*

Follow this and additional works at: <https://louis.uah.edu/honors-capstones>

---

### Recommended Citation

Davis, Dakota Michael, "Mining Optical Narrow-Band Imaging Data to Study AGN Feedback and Galaxy Evolution" (2024). *Honors Capstone Projects and Theses*. 881.

<https://louis.uah.edu/honors-capstones/881>

This Thesis is brought to you for free and open access by the Honors College at LOUIS. It has been accepted for inclusion in Honors Capstone Projects and Theses by an authorized administrator of LOUIS.

# Mining optical narrow-band imaging data to study AGN feedback and galaxy evolution

by

**Dakota Michael Davis**

An Honors Capstone

submitted in partial fulfillment of the requirements

for the Honors Certificate

to

The Honors College

of

The University of Alabama in Huntsville

4/28/2024

Honors Capstone Project Director: Dr. Ming Sun



4/27/2024

---

Student (signature)

Date



04/27/2024

---

Project Director (signature)

Date

---

Department Chair (signature)

Date

---

Honors College Dean (signature)

Date



Honors College

Frank Franz Hall

+1 (256) 824-6450 (voice)

+1 (256) 824-7339 (fax)

honors@uah.edu

### Honors Thesis Copyright Permission

**This form must be signed by the student and submitted with the final manuscript.**

In presenting this thesis in partial fulfillment of the requirements for Honors Diploma or Certificate from The University of Alabama in Huntsville, I agree that the Library of this University shall make it freely available for inspection. I further agree that permission for extensive copying for scholarly purposes may be granted by my advisor or, in his/her absence, by the Chair of the Department, Director of the Program, or the Dean of the Honors College. It is also understood that due recognition shall be given to me and to The University of Alabama in Huntsville in any scholarly use which may be made of any material in this thesis.

Dakota Davis

Student Name (printed)

Dakota Davis

Student Signature

4/27/2024

Date

# Table of Contents

<b>Table of Contents</b> .....	<b>1</b>
<b>Abstract</b> .....	<b>2</b>
<b>Introduction</b> .....	<b>3</b>
Analysis & Calculations.....	5
Data Analysis.....	5
Seeing & Scattering.....	7
<b>Image Generation</b> .....	<b>10</b>
Time Constants.....	10
Aligning & SWarp.....	12
<b>Conclusions</b> .....	<b>14</b>
<b>References</b> .....	<b>15</b>
<b>Appendix A</b> .....	<b>16</b>
<b>Appendix B</b> .....	<b>17</b>
<b>Appendix C</b> .....	<b>18</b>
<b>Appendix D</b> .....	<b>19</b>

## **Abstract**

While modern wide-field optical surveys have routinely imaged the whole sky in broad bands, wide-field narrow-band imaging centered on bright emission-lines has been little explored. Recent surprising discoveries on the giant emission-line clouds around M31 and M82 are good examples to demonstrate the potential of wide-field narrow-band imaging. In this project, I will reduce the recent narrow-band imaging data from the 90Prime instrument of the Bok telescope. I will search for and study features significant in narrow bands to study AGN feedback and galaxy evolution. Multi-wavelength supporting data will also be examined.

## Introduction

The discovery of a “faint. . . [O III] filamentary emission arc” in M31 and “an H $\alpha$ -emitting filament of gas. . . along with a unique large H $\alpha$ -emitting clump” in M82 by has demonstrated the potential of wide-field narrow-band imaging [1] [2]. I will further explore its potential by analyzing and reducing data collected from the Bok telescope at The Kitt Peak National Observatory. With this data, I aim to look for diffuse optical emission-line nebulae/filaments to reveal the feedback from the central supermassive black holes in giant elliptical galaxies. To do so, I will be analyzing the quality of the collected data, calculating the seeing and scattering, and calculating time constants for SWarp image generation.

The data I worked with in this project was collected by my peer, and fellow member of the research group, over the course of January 5th - 14th at The Kitt Peak National Observatory. The “Kitt Peak National Observatory is located on Kitt Peak of the Quinlan Mountains in the Arizona-Sonoran Desert on the Tohono O'odham Nation” [3]. The data was collected using the UArizona Bok 2.3-meter Telescope’s 90Prime wide-field imager. The Bok Telescope has a primary mirror clear aperture of 90 inches in diameter, a primary focal ratio of f/2.66, and a 1.5 arcsecond field of view [3][4]. Across the collection period, data was collected with an R-band filter along with six different Narrow-band filters, including KP1494, KP1495, KP1496, KP1497, KP1517, and KP1566.

For this project, I used five different programs: SAOImageDS9, Image Reduction and Analysis Facility (IRAF), Fv, FTOOLS and SWarp. The quality analysis of the Bok Telescope data will primarily be done using DS9; however, I would later use IRAF to get data required to calculate the seeing and scattering for the data. The time constants were calculated from DS9 image data, and these constants were later used for generating images using SWarp (a program

that co-adds FITS files). Some alignment corrections needed to be made using Fv (a FITS file editor) prior to SWarp image generation.

## Analysis & Calculations

### Data Analysis

To begin, the Bok Telescope data was put through a visual analysis in DS9. Data was organized by date collected and by which object it was collected for. Each image was open as a Mosaic WCS along with the 'b' color option and then set to 'square root' and '99.5%' scale, for better contrast. The data was then visually inspected by finding a star, drawing a circular region over its center, and adjusting the contrast to determine if the image is in focus or not (then labeled accordingly). For an image with good focus, the star would form symmetrically within the region as the contrast is adjusted; this method and trait is exhibited by the star in Figure 1.

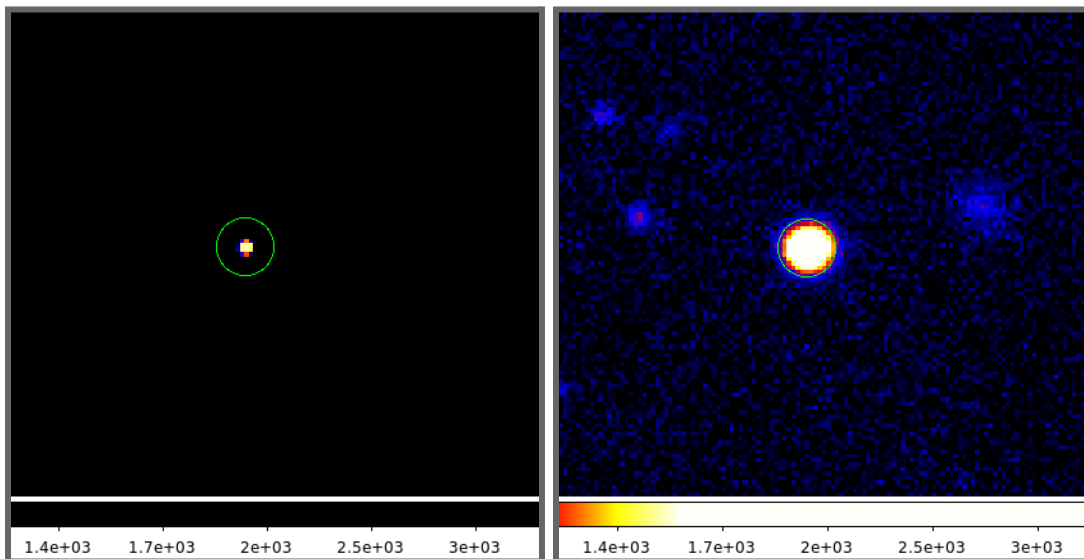


Figure 1: Example of an image with good focus. The star is symmetric within the region placed around its center after contrast adjustment.

Alternatively, for an image with bad focus, the star would form asymmetrically in the region or appear stretched, as demonstrated by the examples in Figure 2. Unfortunately, after the visual inspection of the ~350 image files, roughly half had bad focus (see Appendix A).



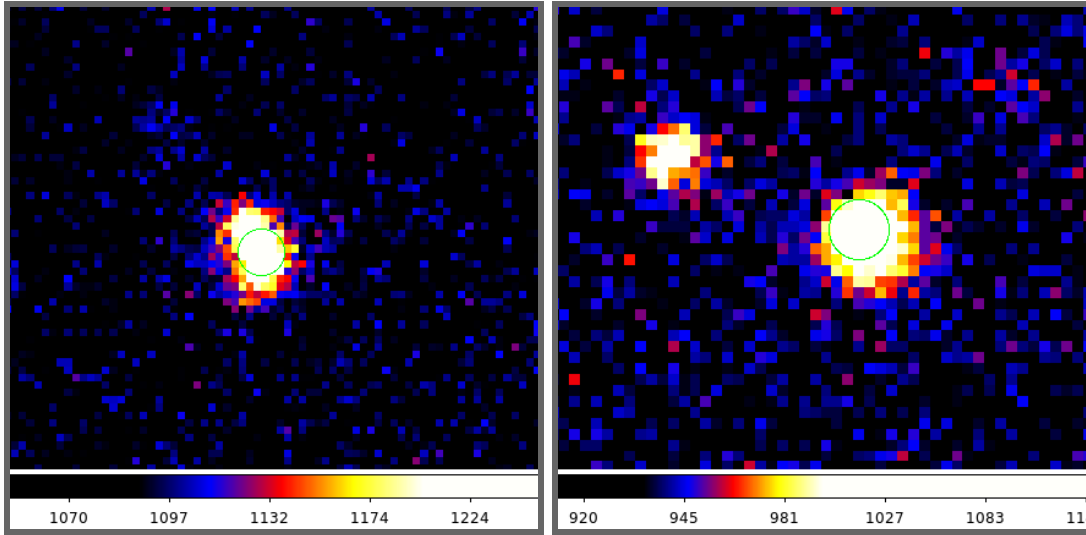


Figure 2: Examples of images with bad focus. The left image's star appears stretched while the right's star is asymmetric around the region.

In addition to labeling the images as having good or bad focus, notes were taken on any other important features found in the image, such as fringes. Fringes, as seen in Figure 3, are wavy features that may appear on the image and look like alternating lighter and darker bands. Fringing appeared most often in data taken with the KP1517 Narrow-band filter. It should be noted that the presence of fringes does not automatically make data bad; however, fringes do cause more difficulty during the data reduction process.

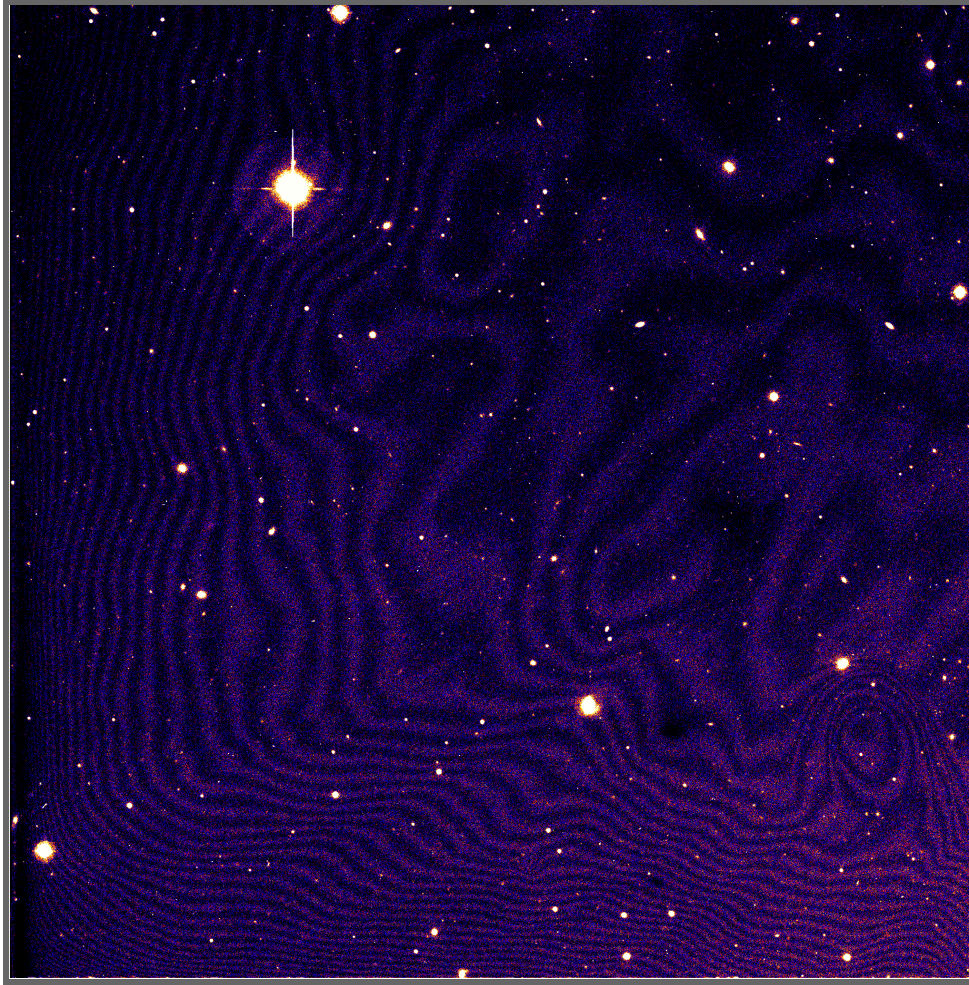


Figure 3: Example of an image with obvious fringing.

## Seeing & Scattering

Next, a small selection of the data with good focus was reduced by an associate at NOIR Lab to be used for further analysis, calculations, and image generation. Of the selection of reduced data, 18 files had Narrow and R-band pairs. These 18 file pairs are what were used for the remainder of the project since both band files were necessary for SWarp image generation. The values to be calculated next were the average seeing and scattering was calculated for each reduced data image. The seeing is a measure of an image's sharpness, or how affected the image is by turbulence in the Earth's atmosphere [6]. A lower seeing relates to a sharper image, so a

lower seeing is preferred. The scattering, or standard deviation of the individual seeing values, is a measure of the seeing's dispersion. In other words, the scattering is a measure of how much the seeing throughout the image differs from the average seeing. So, a lower scattering is preferred since it points towards a more uniform image. To calculate these values, the selection of reduced data was individually loaded into IRAF and IRAF's 'imexamine' (imexam) capabilities were used to retrieve the values to be used in calculating the seeing and scattering for the image. Once the image was loaded, five stars were chosen and the Aperture Radial Photometry Measurement table, or a-key table, was used to display information about a chosen star. An example of the a-key table can be seen in Figure 4.

#	COL	LINE	COORDINATES		PEAK	E	PA	BETA	ENCLOSED	MOFFAT	DIRECT
#	R	MAG	FLUX	SKY							
3444.05	3749.48	3444.05	3749.48		0.9583	0.19	85	3.78	8.45	8.13	7.92
	23.74	20.08	92.97	0.6839							

Figure 4: Example of the table produced by the Aperture Radial Photometry Measurement function in IRAF.

The primary value needed for calculation was the full-width half maximum (FWHM) in pixels, which is noted by the blue box in Figure 4. Additionally, the profile fit peak, within the red box in Figure 4, was useful in choosing the five stars to calculate the average seeing and scattering from, as the stars chosen should not be saturated (wanted a peak ~1.5) [5].

After the FWHM was collected for each of the five chosen stars, the equation

$$Seeing = FWHM \text{ in pixels} * \left( \frac{Region \text{ Radius in wcs-arcsec}}{Region \text{ Radius in pixels}} \right)$$

was used to calculate the seeing. The pixel scale (the term in parentheses) was found by drawing a 10-pixel radius, circular region around the star, then converting the region to arcseconds to find the arcseconds per pixel. The pixel scale for these images was calculated to be 0.25 arcseconds per pixel. An average of the five seeing values was taken to represent the image's seeing. The scattering was then calculated by using the following equation.

$$scattering = \sqrt{\frac{\Sigma(x_i - \bar{x})^2}{n-1}}$$

Here,  $x_i$  is the individually calculated seeing,  $\bar{x}$  is the average seeing, and  $n$  is the number of individual seeings calculated.

These average seeing and scattering values reflect the quality of the data they were calculated from. The typical seeing for the Bok Telescope is 1.5" [4]. However, only 16 of the 36 total reduced data had an average seeing below 2", with the rest having an average seeing greater than 2" (see Appendix B). The higher seeing values are likely due to poor focus potentially caused by temperature fluctuations at the telescope site, and were more commonly found in R-band images.

# Image Generation

## Time Constants

The next process to be done with the reduced data was to make SWarp images by co-adding the matching Narrow and R-band files. To make these images, a time constant needed to be calculated in order to scale down the flux of the R-band image for subtraction from the Narrow-band image. An average time constant was calculated for each image, taken from time constants of five chosen stars of similar brightness. The flux values measured in order to calculate the time constants were taken via the Region Analysis feature in DS9, and the time constant, itself, is a ratio of fluxes calculated via aperture photometry.

To calculate this time constant, a circular region was drawn over a chosen star in both Narrow and R-band images, and the region's flux and area were measured in both ( $C_1$  and  $A_1$ ). Then, a region of the same size was drawn over the background nearby, and similarly the flux and region area were measured in both images ( $C_2$  and  $A_2$ ). A representation of this process can be seen in Figure 5 (a and b). A region of the same size was used since it made value collection and calculations simpler. Once both the star region and background flux was measured, the following equation was used to calculate the star's flux in both band images.

$$\text{total flux of the star, } C = C_1 - \left(\frac{A_1}{A_2}\right)C_2$$

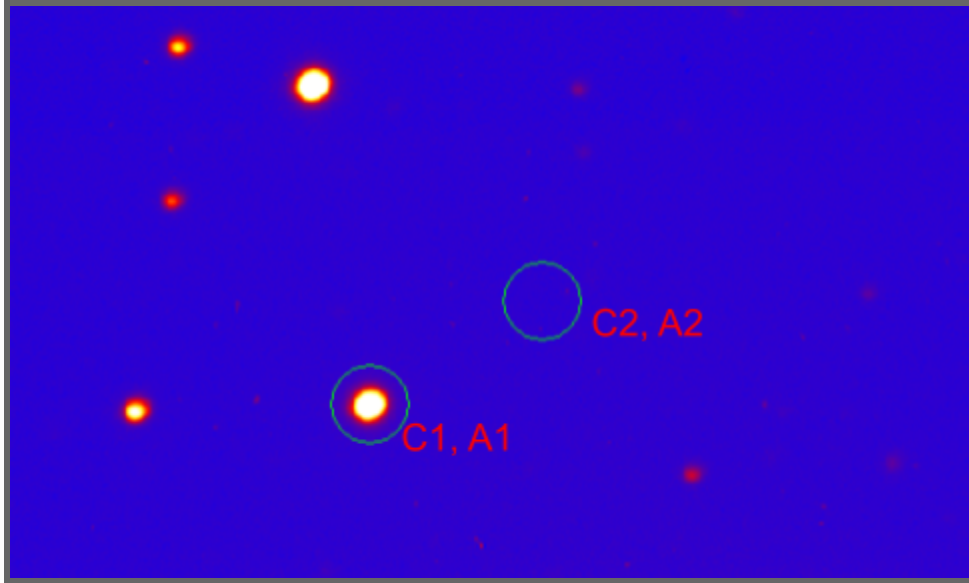


Figure 5a: Sample image of the regions drawn over a star and background used in the time constant calculation.

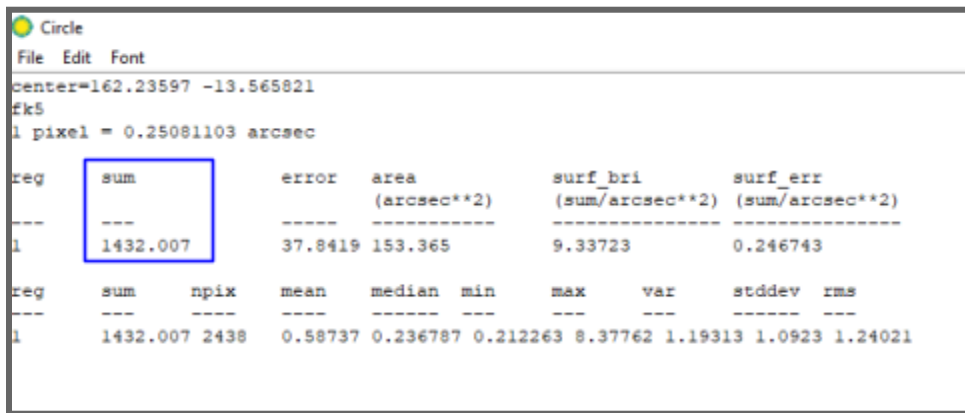


Figure 5b: Sample of the Region Analysis window for C1,A1 where the flux of the star region is highlighted

Once the star's flux had been calculated in each the Narrow-band and R-band image, the following ratio of fluxes is used to generate the time constant.

$$time\ constant = \frac{total\ flux\ of\ star\ in\ Narrow\ band}{total\ flux\ of\ star\ in\ R\ band}$$

For each pair of Narrow-band and R-band images, five time constants were calculated and an average time constant was calculated to represent the image pair (see Appendix C). These time constants were then used to scale the R-band files for SWarp image generation.

## **Aligning & SWarp**

The next step in the image generation process was to multiply the R-band files by their corresponding average time constant using the ‘fcarith’ function of FTOOLS, a general software used to manipulate FITS files [7]. However, the Bok Telescope data needed to be aligned with the cataloged location of the image’s object/galaxy.

To align the images, the file header data needed to be modified. To determine the values to modify, the Narrow-band and R-band image pairs were opened in DS9 and a new frame was created for the 2MASS image server. Once the 2MASS image server was loaded for the specified object, a catalog search was performed and the 2MASS All Sky Catalog of Point Sources was selected to overlay the location of stars onto the Narrow-band and R-band images (see Appendix D (a,b,c)). To align the image, a star near the object was selected, and its location in three different forms were noted: the 2MASS coordinates in degrees, the Narrow-band image coordinates, and the R-band image coordinates. The file headers were then opened using Fv, and the values for CRVAL1, CRVAL2, CRPIX1, and CRPIX2 were edited. The CRVAL1 and CRVAL2 values were adjusted to the 2MASS coordinates of the selected star while the CRPIX1 and CRPIX2 values were adjusted to the image coordinates for its respective band image (Narrow and R)

Once the reduced data files were aligned, the R-band files were multiplied by the negative time constant. Then, to make the co-added image, the Narrow-band file and the newly scaled R-band file were run through SWarp. The SWarp image generation process produced a

new image in which the Narrow-band file was subtracted from by the scaled R-band file in the relation below.

$$\text{Narrow band} - (\text{time constant} * \text{R band})$$

Two examples of SWarp images generated from the reduced Bok Telescope data can be seen in Figure 6 (a,b). This process of subtraction and the generating SWarp images was done to potentially reveal H $\alpha$  and [N II] emission regions.

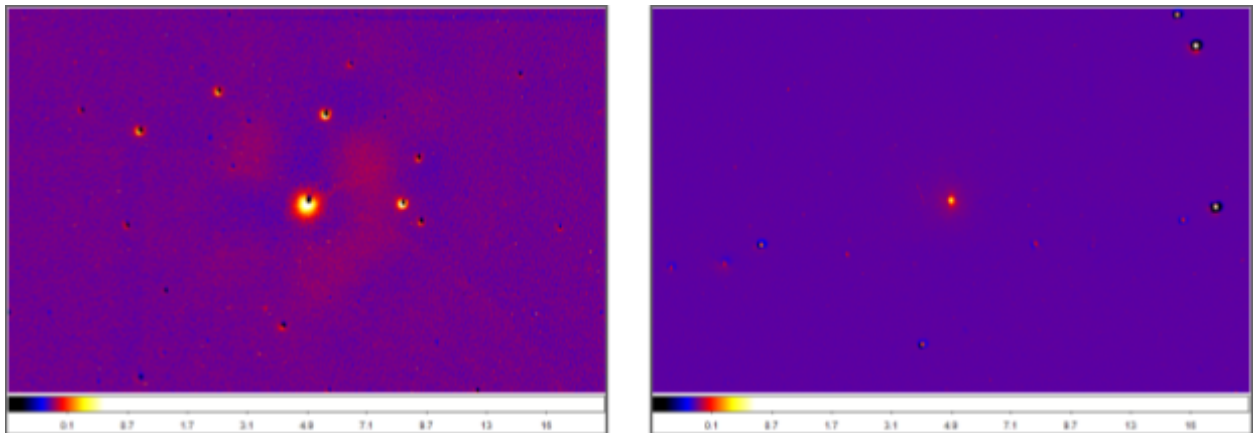


Figure 6: Examples of SWarp images made from the reduced Bok Telescope data set. Left (6a) is of NGC777, while right (6b) is of NGC3402



## Conclusions

Due to time constraints, a full analysis of the SWarp images was unable to be completed. However, a preliminary analysis of the NGC3402 image has not revealed any points of interest. SWarp images were generated for each of the image file pairs, though, so further research projects could be done to further analyze the Bok Telescope data and the SWarp images generated from it. Furthermore, only a sample of the data gathered across the data collection period at the Kitt Peak National Observatory was reduced for use in this project. Thus, further work could be done to reduce more of the Bok Telescope data as well as perform additional calculations for seeing, scattering, and generation of SWarp images for analysis.

Although, even after aligning the image pairs via  $F_v$ , many of the SWarp images had noticeable alignment issues. This is mainly due to inaccuracies in the relative astronomy between the Narrow and R-band images, and is exacerbated by the different seeing and focus of the Bok Telescope data. So, this is an issue to keep in mind when considering future work with this data.

## References

- [1] Drechsler, Marcel, et al. "Discovery of Extensive [O III] Emission near M31." *Research Notes of the AAS*, vol. 7, no. 1, 4 Jan. 2023, p. 1, doi:10.3847/2515-5172/acaf7e.
- [2] Lokhorst, Deborah, et al. "A Giant Shell of Ionized Gas Discovered near M82 with the Dragonfly Spectral Line Mapper Pathfinder." *The Astrophysical Journal*, vol. 927, no. 2, 1 Mar. 2022, p. 136, doi:10.3847/1538-4357/ac50b6.
- [3] NOIR Lab, "UArizona Bok 2.3-Meter Telescope." *NOIRLab*, noirlab.edu/public/programs/kitt-peak-national-observatory/bok-telescope/. Accessed 27 Apr. 2024.
- [4] Schmidt, Gary, and Paul Smith. *Bok Telescope and Site*, james.as.arizona.edu/~psmith/90inch/90tel.html. Accessed 27 Apr. 2024.
- [5] "Iraf Imexamine Capabilities." *IRAF Imexamine Capabilities - Imexam v0.1.Dev53+gebea0bb*, imexam.readthedocs.io/en/latest/imexam/iraf\_imexam.html. Accessed 27 Apr. 2024.
- [6] "Seeing." *Encyclopædia Britannica*, Encyclopædia Britannica, Inc., www.britannica.com/science/seeing. Accessed 27 Apr. 2024.
- [7] "FTOOLS." *NASA*, heasarc.gsfc.nasa.gov/lheasoft/ftools/ftools\_menu.html. Accessed 27 Apr. 2024.

# Appendix A

## A

The link(s) below are to a pdf of the spreadsheet of the visual analysis and notes on the Bok Telescope data. Analysis and notes were made in a spreadsheet form due to the large number of files that needed to be analyzed.

 Bok Data Analysis - Dakota Davis - Sheet1.pdf

<https://drive.google.com/file/d/1DuE5EzU5RaN9Wl44P3rXwMxVBnshFzKd/view?usp=sharing>

## Appendix B

### Seeing & Scattering Calculations for Reduced Bok Data

The link(s) below are to a pdf of the spreadsheet of the values used in the calculation of the seeing and scattering, as well as the calculated of the seeing and scattering themselves.

Calculations were done using the function feature of the spreadsheet, and were automatically calculated using the formulas mentioned in the paper above.

■ Seeing and Scattering Calculations for Reduced Bok Data - Sheet1.pdf

<https://drive.google.com/file/d/1ifEJEdrsZAofmUNvMP4ifVXJ0XO1jhTl/view?usp=sharing>

## Appendix C

### Time Constant Measurements (Bok data)

The link(s) below are to a pdf of the spreadsheet of the values used in the calculation of the time constants, as well as the calculated of the time constants themselves. Calculations were done using the function feature of the spreadsheet, and were automatically calculated using the formula mentioned in the paper above.

📄 Time\_Constant\_Measurements (Bok data) - Sheet1.pdf

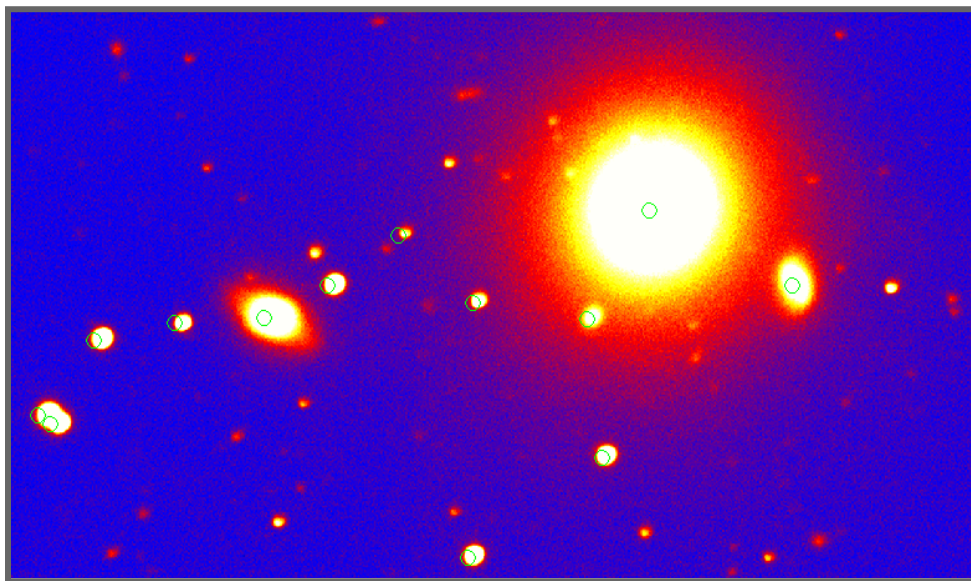
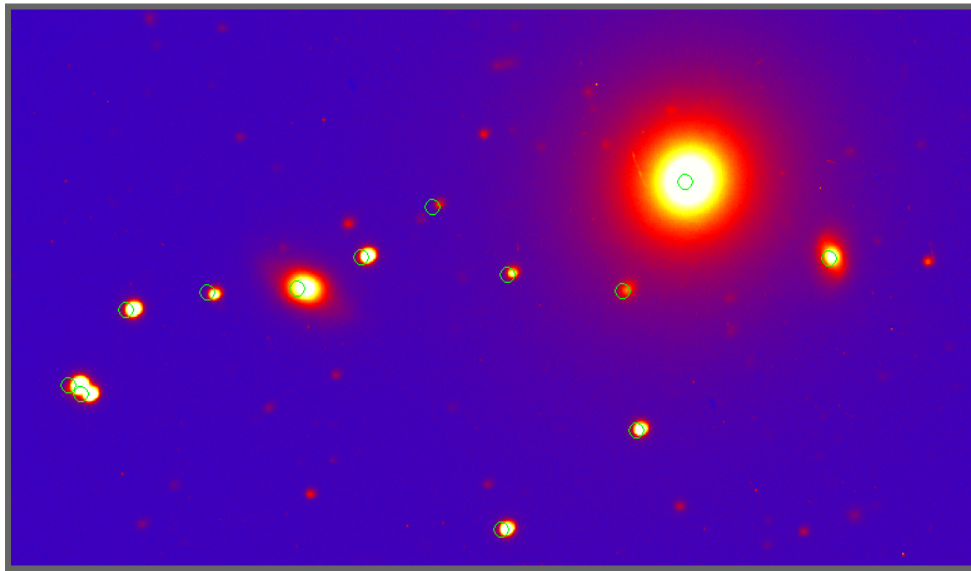
<https://drive.google.com/file/d/1EuBoK9oSQuhpdE2pDYYIFn1VKzWdDV/view?usp=sharing>

g

## Appendix D

### Narrow-band & R-band images of NGC3402 with 2MASS overlay in DS9

The three frames (Narrow (a), R (b), 2MASS (c)) of the NGC3402 file pair opened in DS9 with the 2MASS All Sky Catalog of Point Sources overlay applied to both the Narrow-band and R-band frames.



## Appendix D (Continued)

